A grounded-load charge amplifier for reducing hysteresis in piezoelectric tube scanners

A. J. Fleming[a] and S. O. R. Moheimani
The School of Electrical Engineering and Computer Science, The University of Newcastle, Callaghan 2308, Australia

(Received 11 January 2005; accepted 1 May 2005; published online 29 June 2005)

In this paper, a charge amplifier adapted for piezoelectric tube scanners is presented. Previous problems involved with the implementation of such amplifiers are resolved to provide dc accurate performance with zero voltage drift. In our experiment, hysteresis was reduced by 89% when compared to a voltage amplifier. © *2005 American Institute of Physics.* [DOI: 10.1063/1.1938952]

I. INTRODUCTION

Piezoelectric tube scanners were reported by Binnig and Smith[1] for use in scanning tunneling microscopes.[2] They were found to provide a higher positioning resolution and greater bandwidth than traditional tripod positioners while being simple to manufacture and easier to integrate into a microscope. Piezoelectric tube scanners are now used extensively in scanning probe microscopes and many other applications requiring precision positioning, e.g., nanomachining,[3,4] etc.

As shown in Fig. 1(a), a piezoelectric scanner comprises a tube of radially poled piezoelectric material with four external electrodes and a grounded internal electrode. Other configurations may include a circumferential electrode for independent vertical extension or diameter contraction. The internal electrode may also be sectored. Small-deflection expressions for the lateral tip translation were presented by Chen.[5]

Nonlinearity has been an ongoing difficulty associated with piezoelectric tube scanners (and piezoelectric actuators in general). When employed in an actuating role, piezoelectric transducers display a significant hysteresis in the transfer function from an applied voltage to resulting strain or displacement.[6] Due to hysteresis, ideal scanning signals can result in severely distorted tip displacements and hence poor image quality or poor reproducibility.

Techniques aimed at addressing both mechanical dynamics and hysteresis can be grouped generally into two broad categories: feedforward and feedback. Feedforward techniques, as shown in Fig. 1, do not include a sensor but require accurate knowledge of the undesirable dynamics. Feedback systems, although more robust to modeling error, are limited by the noise performance and bandwidth of the sensor. In many cases it is also difficult and/or prohibitively expensive to integrate displacement sensors into the scanning apparatus.

Feedforward and signal compensation approaches have been studied extensively as their implementation requires no additional hardware or sensors. It should be considered, however, that additional hardware such as displacement sensors and digital signal processors are required to identify the behavior of each tube prior to implementation. A technique for designing optimal linear feedforward compensators was presented by Croft and co-workers,[7] then later extended to incorporate a PD feedback controller.[3] In these works, the authors identify the main limitation to performance as being modeling error. Another feedforward technique, known as iterative or learning control is aimed at reducing unmodeled hysteresis. The need for a model is essentially annulled with the use of a sensor and online iteration to ascertain the optimal input compensation.[8] The foremost problems with iterative techniques are the time taken to iterate the compensator and difficulties associated with nonmonotonic trajectories. Other feedforward approaches have included: model-based hysteresis inversion,[9,10] optimal $\mathcal{H}_\infty$ compensation,[11] compensation for creep, Preisach hysteresis and resonance,[12] improved iterative Preisach inversion,[13] and various optimal linear feedforward compensation techniques.[14,15]

Feedback techniques can provide excellent low-frequency tracking performance, but depend heavily on the sensor noise performance and bandwidth. As a consequence, such techniques are most applicable to scan ranges in the hundreds of nanometers or greater. Good tracking of a 5-Hz triangle wave, while maintaining robustness to nonlinearity was presented by Salapaka *et al.*[16] With the integration of displacement sensors into the next generation of commercial microscopes, feedback systems will become more feasible.

Considering the breadth of research aimed at improving scan performance, it is surprising to find that commercial microscope manufacturers have been reluctant to adopt the techniques discussed. The majority of commercial scanning systems operate in much the same fashion as they did in the early 1990s. Regardless of the potential benefits, the requirement for data acquisition, sophisticated modeling experiments, and additional sensors have severely limited the application of feedforward and feedback scan compensation. With this in mind, the research in this paper presents a simple non-model-based technique for the reduction of hysteresis.

Since the late 1980s, it has been known that driving

[a]Electronic mail: andrew.fleming@newcastle.edu.au

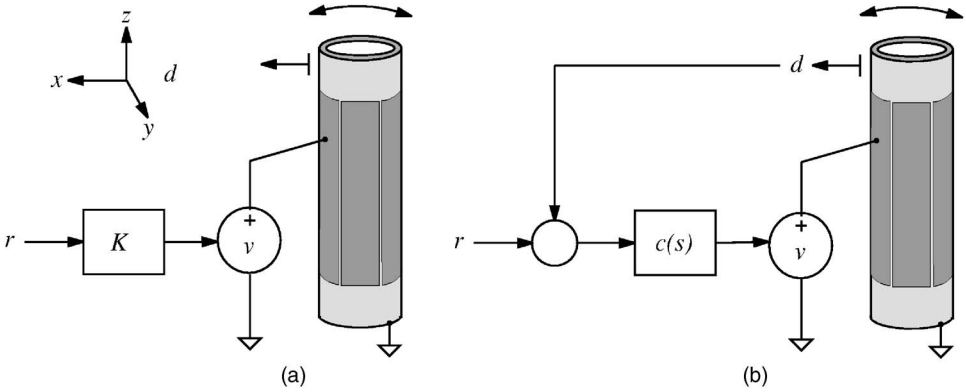

FIG. 1. Voltage driven tube scanner. (a) Open loop with signal precompensation. (b) Closed loop with displacement feedback.

piezoelectric transducers with current or charge rather than voltage significantly reduces hysteresis.[17] Simply by regulating the current or charge, a fivefold reduction in the hysteresis can be achieved.[18] However, this technique is not without difficulties:[19] While hysteresis in a piezoelectric actuator is reduced if the charge is regulated instead of the voltage,[17] the implementation complexity of this technique prevents a wide acceptance.[20]

Although the circuit topology of a charge or current amplifier is much the same as a simple voltage feedback amplifier, the uncontrolled nature of the output voltage typically results in the load capacitor being charged up. Saturation and distortion occur when the output voltage, referred to as the compliance voltage, reaches the power supply rails. The stated *complexity* invariably refers to the need for additional circuitry to avoid charging of capacitive loads.

In this paper, a class of grounded-load charge amplifier free from dc and low-frequency voltage drift is presented. The design, motivated by a discussion of previous problems, is introduced in Sec. II. Experimental results in Sec. III report 89% hysteresis reduction and successful low-frequency scanning of a piezoelectric tube. Conclusions follow in Sec. IV.

II. DC ACCURATE CHARGE AMPLIFIER

Consider the simplified diagram of a generic current source shown in Fig. 2. The piezoelectric load, modeled as a capacitor and voltage source v_p, is shown in gray. The high gain feedback loop (k_C) works to equate the applied reference voltage v_{ref}, to the voltage across a sensing capacitor

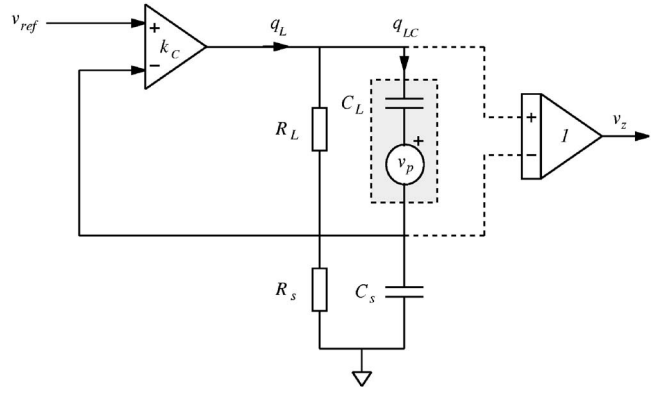

FIG. 2. Simplified diagram of a generic charge source.

C_s. Neglecting the resistances R_L and R_s, at frequencies well within the bandwidth of the control loop, the load charge q_L is equal to

$$q_L = V_{\text{ref}} C_s, \tag{1}$$

i.e., we have a charge amplifier with gain C_s Columbs/V.

The foremost difficulties associated with the charge amplifier shown in Fig. 2 are due to the resistances R_L and R_s. These resistances model the parasitic leakage resulting from the input terminals of the feedback opamps, capacitor dielectric leakage, and v_z measurement. In practice, this parasitic resistance is often swamped with additional physical resistances required to manage voltage drift associated with the input bias current of the opamps and voltage instrumentation.

If there exists a parallel load resistance R_L, the actual charge $q_{Lc}(s)$ flowing through the load transducer becomes

$$q_{LC}(s) = q_L(s) \frac{s}{s + \dfrac{1}{R_L C_L}}. \tag{2}$$

The amplifier now contains a high-pass filter with cutoff $\omega_c = 1/R_L C_L$. That is,

$$\frac{q_{LC}(s)}{V_{\text{ref}}(s)} = C_s \frac{s}{s + \dfrac{1}{R_L C_L}}. \tag{3}$$

In a typical piezoelectric tube drive scenario, with $C_L = 10$ nF, a 1-μA output offset current requires a 10-MΩ parallel resistance to limit the dc voltage offset to 10 V. Phase lead exceeds 5 deg. below 18 Hz. Such poor low-frequency performance precludes the use of charge amplifiers in applications requiring accurate low-frequency tracking, e.g., atomic force microscopy.[21]

A solution to the problem of voltage drift was presented in a previous publication.[22] An auxiliary voltage feedback loop was included to correct low-frequency behavior and allow for constant charge offsets. The circuit implementation required the design of separate voltage and charge feedback controllers. A simplified design relying on the intrinsic voltage control offered by the parasitic resistances was later presented by Yi and Veillette.[23] Neither of the amplifiers discussed have been capable of driving grounded loads. As piezoelectric tubes have multiple external electrodes and a common (often grounded) internal electrode, the requirement for a grounded load is a necessity.

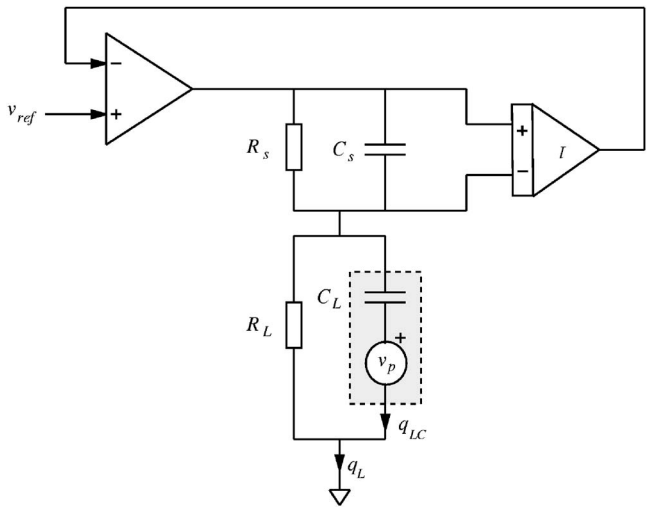

FIG. 3. Grounded load dc accurate charge amplifier.

Following we present the design of a dc accurate grounded-load charge amplifier. Shown in Fig. 3, the amplifier works to equate the voltage measured across the sensing impedance to the reference voltage v_{ref}.

To understand the operation of the amplifier we study the transfer function from the reference voltage v_{ref} to the load charge q_{LC}.

$$\frac{q_L(s)}{v_{\mathrm{ref}}(s)} = C_s \frac{s + \dfrac{1}{C_s R_s}}{s}. \tag{4}$$

The reference to actual load charge transfer function can be found by combining Eqs. (4) and (2)

$$\frac{q_{\mathrm{LC}}(s)}{v_{\mathrm{ref}}(s)} = \frac{q_L(s)}{v_{\mathrm{ref}}(s)} \frac{q_{\mathrm{LC}}(s)}{q_L(s)} = C_s \frac{s + \dfrac{1}{C_s R_s}}{s} \frac{s}{s + \dfrac{1}{R_L C_L}}. \tag{5}$$

By setting $C_L R_L = C_s R_s$, i.e.,

$$\frac{R_L}{R_s} = \frac{C_s}{C_L}, \tag{6}$$

the amplifier has no low-frequency dynamics and constant gain C_s Columbs/Volt. Effectively the voltage amplifier, comprised of the two resistances R_L and R_s, synthesizes the operation of an ideal charge amplifier at low frequencies.

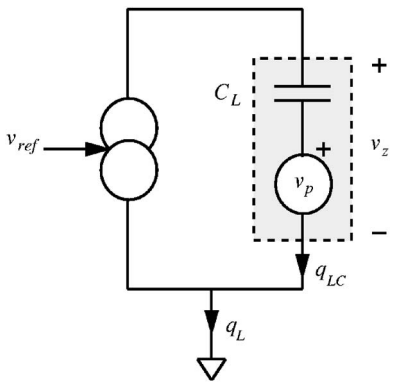

FIG. 4. Test for voltage/charge dominance.

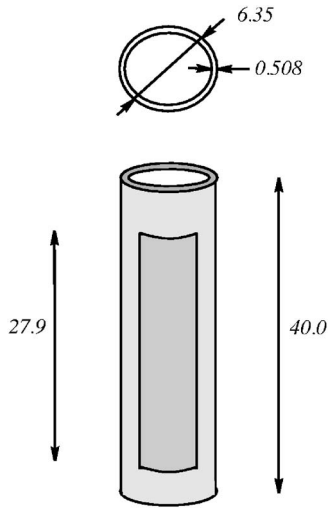

FIG. 5. Piezoelectric tube dimensions (in millimeters).

If the amplifier can be viewed as the concatenation of a voltage and charge amplifier, an important question is: In what regions of operation does the amplifier operate as a pure charge amplifier? Likewise for voltage operation. Consider the schematic shown in Fig. 4. During perfect charge operation, i.e., when q_{LC} is correctly regulated to zero, the voltage v_z will be equal to v_p. During voltage dominant behavior, v_z will be regulated to zero. Such characteristics are easily measured experimentally. Although the voltage dynamics have been designed to synthesize the operation of an ideal charge amplifier, during voltage dominant operation, if the load is not purely capacitive, errors in q_{LC} will occur.

When $v_{\mathrm{ref}}=0$, which implies $q_L=0$, the transfer function from v_p to v_z reveals the voltage or charge dominance of the amplifier. At frequencies where $v_z \approx v_p$, the amplifier is charge dominant, and voltage dominant when $v_z \approx 0$. For the hybrid amplifier shown in Fig. 3, when $v_{\mathrm{ref}}=0$,

$$\frac{v_z(s)}{v_p(s)} = \frac{s}{s + \dfrac{1}{R_L C_L}}, \tag{7}$$

i.e., at frequencies above $1/RC$ s^{-1} the amplifier is charge dominant, and voltage dominant below. Obviously, given Eq. (7), the objective will be to select a load resistor R_L as large as possible. This may be limited by other factors such as opamp current noise attenuation, bias-current-based offset voltages, and the common-mode and differential leakage of the opamp. In practice, $v_z(s)/v_p(s)$ is best measured by simply applying a voltage to another electrode and using that as a reference, as the frequencies under consideration are well below the tube's mechanical resonance, the applied voltage will be related by a constant.

III. EXPERIMENTAL RESULTS

In this section, the prototype shunt circuit and charge amplifier are employed to drive a piezoelectric tube positioner in one dimension. Further details on the amplifier electronics or commercially available devices are freely available

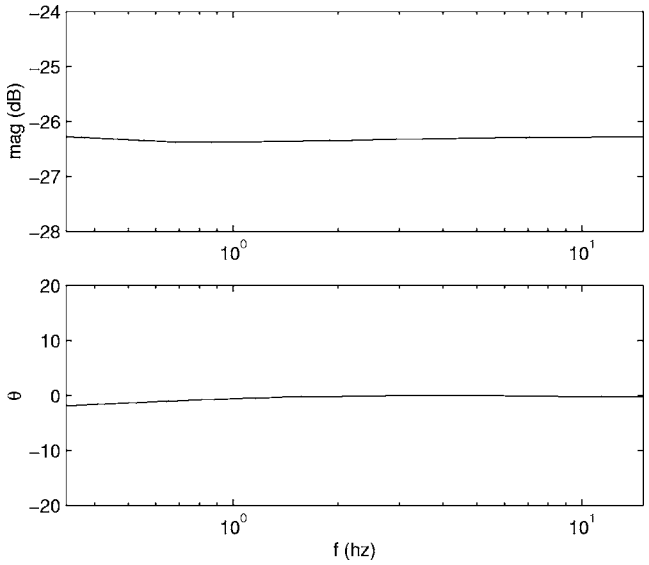

FIG. 6. Charge amplifier low-frequency tracking performance. Measured from the charge reference signal (V) to the instrumented load voltage across a 5-nF dummy load.

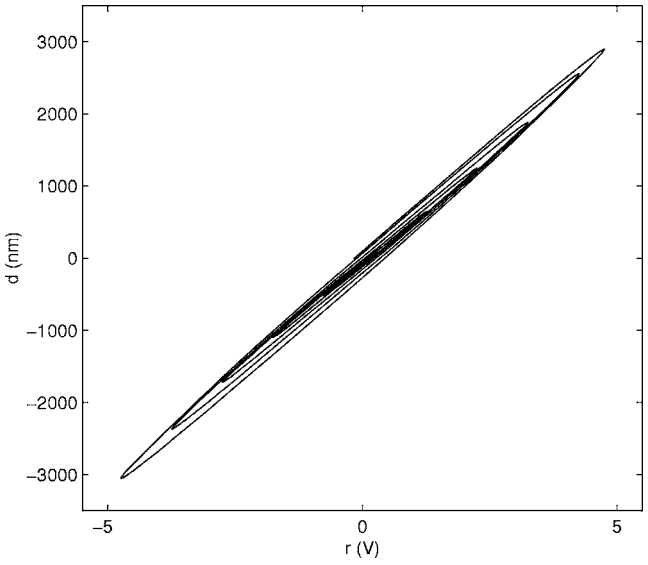

FIG. 8. Relationship between an applied voltage and the resulting tube displacement. (10 Hz ramped sinusoidal input).

by contacting the first author. Physical dimensions of the tube can be found in Fig. 5. An ADE Tech capacitive sensor was used to measure the displacement with sensitivity 10 V/μm and bandwidth 10 kHz. An aluminium cube ($1\times1\times1$ cm^3) is glued onto the tube tip and grounded to provide a return for the capacitive sensor. The charge amplifier has a gain of 77.8 nC/V.

We examine the two characteristics of foremost importance: low frequency charge regulation—the ability of the amplifier to reproduce low-frequency inputs without drift and the bandwidth of charge dominance—the frequency range where hysteresis will be reduced due to dominant charge feedback.

The (low-frequency) transfer function measured from an applied reference signal to the actual charge deposited on a 5- nF dummy load is shown in Fig. 6. Excellent low-frequency tracking from 15 mHz to 15 Hz is exhibited by the amplifier and instrumentation. As discussed in Sec. II, the bandwidth of charge dominance was ascertained by zeroing the charge reference and introducing an internal load voltage. The transfer function measured from the internal voltage to the voltage measured across the load is shown in Fig. 7. We observe a charge-dominance bandwidth of 0.8 Hz. Frequencies above this bandwidth will experience the full linearity benefit of charge actuation.

To justify the use of charge actuation we demonstrate the benefit in Figs. 8 and 9. Hysteresis is reduced by approximately 89% simply through the use of a charge amplifier. Percentage reduction is calculated by $100\times(1-\delta c/\delta v)$, where δc and δv are the charge and voltage driven maximum excursions from linear. It should be noted that a scan range

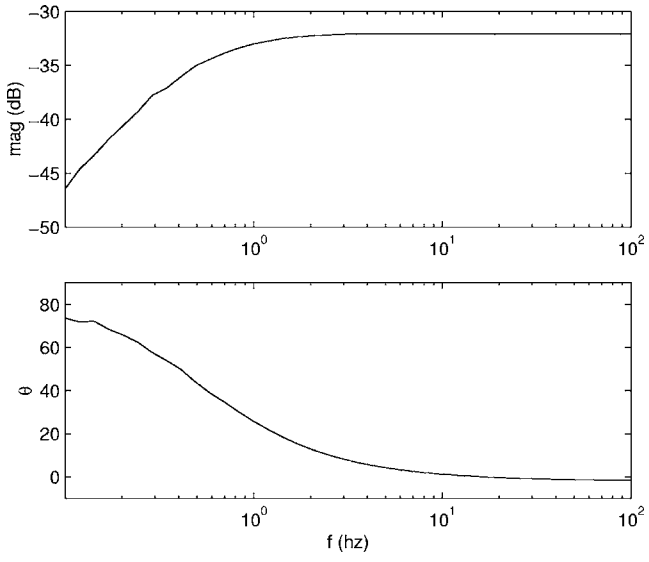

FIG. 7. Charge dominance bandwidth. Measured from the internal tube strain voltage v_p to the load voltage.

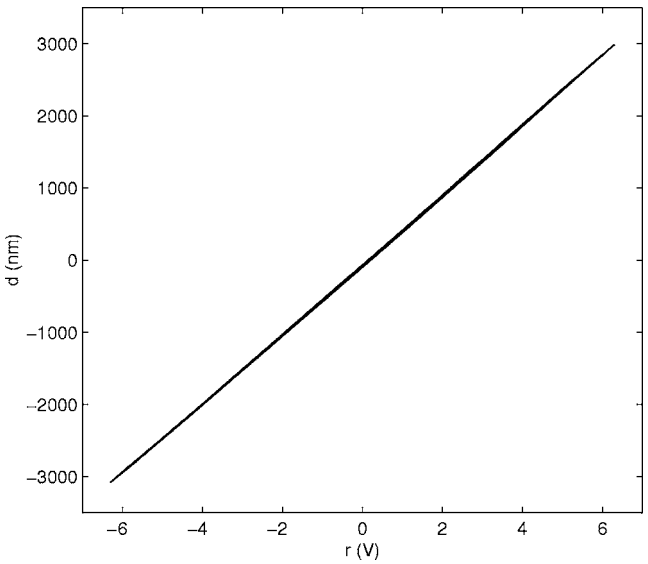

FIG. 9. Relationship between an applied charge reference and the resulting tube displacement. (10-Hz ramped sinusoidal input).

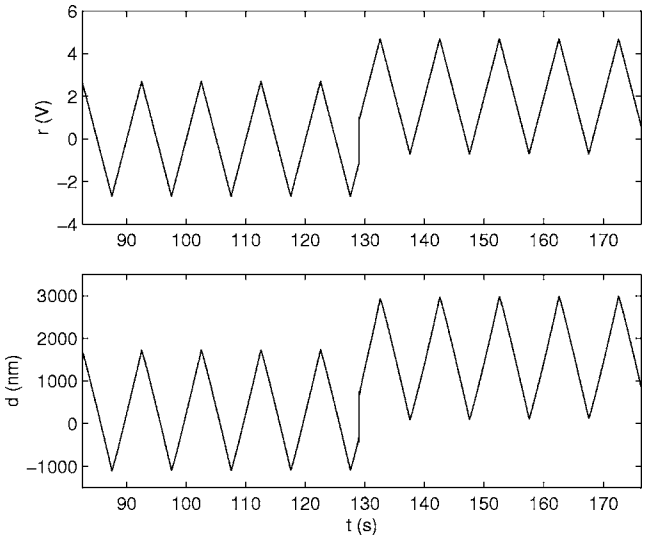

FIG. 10. Low-frequency scanning reference and resultant tube displacement with additive DC offset.

of ±3 μm is around 20% of the full scale deflection, it is often assumed that hysteresis is negligible at such low drives. Similar plots for the same apparatus with a ±8-μm drive can be found in another work,[22] a greater hysteresis is exhibited, and similarly reduced through the use of charge drive.

In Fig. 10 a low-frequency triangle signal was applied to the charge amplifier. At time 130 s a dc offset equivalent to around 1 μm was applied. Aside from the faithful reproduction of a 0.1-Hz triangle wave, the charge amplifier reproduces the offset without drift.

IV. FUTURE RESEARCH

Future research includes the incorporation of the presented amplifier into a scanning tunneling and atomic force microscope. To allow routine image comparisons between microscopes with charge and voltage driven tubes, the amplifier requires offset functionality and variable gain.

[1] G. Binnig and D. P. E. Smith, Rev. Sci. Instrum. **57**, 1688 (1998).
[2] E. Meyer, H. J. Hug, and R. Bennewitz, *Scanning Probe Microscopy* (Springer, Heidelberg, Germany, 2004).
[3] D. Croft, D. McAllister, and S. Devasia, Journal of Manufacturing Science and Technology **120**, 617 (1998).
[4] W. Gao, R. J. Hocken, J. A. Patten, J. Lovingood, and D. A. Lucca, Precis. Eng. **24**, 320 (2000).
[5] C. J. Chen, Appl. Phys. Lett. **60**, 132 (1992).
[6] H. J. M. T. A. Adriaens, W. L. de Koning, and R. Banning, IEEE/ASME Trans. Mechatron. **5**, 331 (2000).
[7] D. Croft, S. Stilson, and S. Devasia, Nanotechnology **10**, 201 (1999).
[8] K. Leang and S. Devasia, 42nd IEEE Conference on Decision and Control Maui, HI, December 2003 (unpublished).
[9] C. Wei, H. Zhang, L. Tao, W. Li, and H. Shi, Rev. Sci. Instrum. **67**, 3594 (1996).
[10] S. Hudlet, M. S. Jean, D. Royer, J. Berger, and C. Guthmann, Rev. Sci. Instrum. **66**, 2848 (1995).
[11] G. Schitter, R. W. Stark, and A. Stemmer, Ultramicroscopy **100**, 253 (2004).
[12] D. Croft, G. Shed, and S. Devasia, J. Dyn. Syst., Meas., Control **123**, (2001).
[13] K. J. G. Hinnen, R. Fraanje, and M. Verhaegen, Journal of Systems and Control Engineering **218**, 503 (2004).
[14] G. Schitter and A. Stemmer, Microelectron. Eng. **67–68**, 938 (2003).
[15] H. Perez, Q. Zou, and S. Devasia, J. Dyn. Syst., Meas., Control **126**, 187 (2004).
[16] S. Salapaka, A. Sebastion, J. P. Cleveland, and M. V. Salapaka, Rev. Sci. Instrum. **75**, 3232 (2002).
[17] C. V. Newcomb and I. Flinn, IEEE Electron Device Lett. **18**, 442 (1982).
[18] P. Ge and M. Jouaneh, IEEE Trans. Control Syst. Technol. **4**, 209 (1996).
[19] J. M. Cruz-Hernandez and V. Hayward, IEEE Trans. Control Syst. Technol. **9**, 17 (2001).
[20] H. Kaizuka and B. Siu, Jpn. J. Appl. Phys., Part 2 **27**, 773 (1988).
[21] D. Croft, G. Shedd, and S. Devasia, in Proc. American Control Conference Chicago, Illinois, June 2000, pp. 2123–2128 (unpublished).
[22] A. J. Fleming and S. O. R. Moheimani, in Proc. 3rd IFAC Symposium on Mechatronic Systems Sydney, Australia, September 2004.
[23] K. A. Yi and R. J. Veillette, IEEE Trans. Control Syst. Technol. **13**, 517 (2005).